

# Electrophoretic deposition of titanium/silicon-substituted hydroxyapatite composite coating and its interaction with bovine serum albumin

XIAO Feng-juan(肖凤娟), ZHANG Ying(张 颖), YUN Li-jiang(云立江)

Materials Science and Engineering Department, Shijiazhuang Railway Institute, Shijiazhuang 050043, China

Received 22 February 2008; accepted 4 September 2008

**Abstract:** Silicon-substituted hydroxyapatite ( $\text{Ca}_{10}(\text{PO}_4)_{6-x}(\text{SiO}_4)_x(\text{OH})_{2-x}$ , Si-HA) composite coatings on a bioactive titanium substrate were prepared by electrophoretic deposition technique with the addition of triethanolamine (TEA) to enhance the ionization degree of Si-HA suspension. The surface structure was characterized by XRD, SEM, XRF, EDS and FTIR. The bond strength of the coating was investigated. The results show that the depositing thickness and the images of Si-HA coating can be changed with the variation of deposition time. The XRD spectra of Ti/Si-HA coatings show the characteristic diffraction peaks of HA, and the incorporation of silicon changes the lattice parameter of the crystal. The FTIR spectra shows that the most notable effect of silicon substitution is the decrease of intensities of  $\text{—OH}$  and  $\text{PO}_4^{3-}$  groups with the silicon contents increasing. XRD and EDS element analyses present that the content of silicon in the coating increases with increasing silicon concentration in the suspension. The bioactive  $\text{TiO}_2$  coating formed may improve the bond strength of the coatings. The interaction of Ti/Si-HA coating with BSA is much greater than that of Ti/HA coating, suggesting that the incorporation of silicon in HA is significant to improve the bioactive performance of HA.

**Key words:** titanium; silicon; hydroxyapatite; composite coating; bovine serum albumin

## 1 Introduction

Titanium coated with hydroxyapatite ( $\text{Ca}_{10}(\text{PO}_4)_6(\text{OH})_2$ , HA) can overcome the brittleness and poor mechanical performance of HA, which makes use of both the excellent biocompatibility of HA and high mechanical strength of metallic materials[1–2]. Silicon is one of the trace elements known to be essential in biological processes. The incorporation of silicon in HA is well known to improve the bioactivity of the material [3]. It is desirable for bone ingrowth to proceed as quickly as possible because the stability of the implanted region depends on the formation of a strong mechanical bond between the implant and the surroundings in the body. Si-HA can increase the rate and amount of bone tissues over pure HA[4]. As a calcific agent, silicon enhances the bony growing rate of bioactive prosthetic material. Its importance on bone formation and calcification has been demonstrated through *in vitro* and *in vivo* studies[5–7]. In recent work, silicon-substituted hydroxyapatite was synthesized by hydrothermal

methods, and the Ti/Si-HA coatings were prepared by electrophoretic deposition technique (EPD) using high voltage to drive the suspended Si-HA particles onto titanium substrate[8–10]. The morphology, composition and the interaction of the coating with bovine serum albumin(BSA)were studied.

## 2 Experimental

### 2.1 Preparation of Ti/Si-HA coating

The starting point of the preparation of Ti/Si-HA coating was the synthesis of Si-HA using the precipitation reaction among  $\text{Ca}(\text{NO}_3)_2 \cdot 4\text{H}_2\text{O}$ ,  $(\text{NH}_4)_2\text{HPO}_4$  (molar ratio  $n(\text{Ca})/n(\text{Si+P})=1.67$ ) and  $\text{Si}(\text{CH}_3\text{CH}_2\text{O})_4$  with triethanolamine(TEA) as surfactant. After complete mixing of the reactants for 12 h at 95 °C, and keeping pH at 10.0 by the addition of  $\text{NH}_3 \cdot \text{H}_2\text{O}$  solution, the precipitates were thoroughly rinsed, and filtered, then dried at 25 °C overnight. The suspensions for EPD were prepared by adding 5.0 g of Si-HA powders to 400 mL of *n*-butanol with triethanolamine as dispersion reagent and then dispersed ultrasonically without further aging.

Titanium samples were abraded on 600-grit silicon carbide paper before deposition and were etched with a solution containing 4% hydrofluoric acid and 3% nitric acid, followed by washing in acetone in an ultrasonic bath for 20 min, then washing in distilled water and drying in air at 25 °C [8–10]. Ti and platinum electrode were used as cathode and anode, respectively, and the distance between the two electrodes was 1.0 cm and the work area was about 1 cm<sup>2</sup>. The voltage of direct current power was maintained at 40 V [11]. The conductivity of the suspension was determined by a conductivity meter as a function of the amount of TEA. The Si-HA powders were positively charged moving towards the cathode to deposit. The coated sheets were sintered at 850 °C to improve coating adhesion. After that, Ti/Si-HA coatings were immersed in the 8 mg/mL BSA solution (0.9% NaCl as buffer) for 3 d [12] to study the interaction between them. Then Ti/Si-HA coatings were taken out, rinsed, and dried in air. The scraped powder of Si-HA was characterized.

## 2.2 Characterization

The element contents of HA and Si-HA were determined by X-ray fluorescence spectrophotometer (XRF) (Philips PW-1606) and EDS (VGR-3). The crystal structure was characterized by XRD (D8-Advance). FTIR (330–FTIR) was used to analyze the function group in the crystals before and after interaction of Ti/Si-HA coatings with BSA. The morphology and the thickness of the coatings were observed on SEM (Kyk-2 800). The bond strength of coatings on substrate was tested through electronic multi-purpose tester (CSS-2210) according to the standard of GB T/8642–1988.

## 3 Results and discussion

### 3.1 Electrophoretic deposition mechanism of Ti/Si-HA composite coating

TEA can enhance the conductivity of the Si-HA suspension. Fig.1 shows the conductivity of Si-HA suspension vs the amount of TEA in *n*-butanol. As shown in Fig.1, the conductivity of the solution changes little with the addition of TEA into pure *n*-butanol, which indicates that the ionization degree of TEA in the *n*-butanol is very little. After the addition of Si-HA particles, the conductivity of the suspension increases from 0.76 μS/cm to 3.26 μS/cm. Conductivity can affect the deposition because the electrophoretic motion of the particles is driven by the motion of the charges adhered to the particles [12]. As alcohol is known to behave as proton donors in the presence of organic bases, it can be adsorbed and ionized on the surface of weak alkaline such as Si-HA particles to form charged particles. TEA has three —OH groups with higher protonation degree

in the presence of Si-HA than that without Si-HA and each particle of Si-HA carries three negative charges, which increases ionic charges available by exchanging H<sup>+</sup> between TEA and Si-HA. So, the conductivity of suspensions increases with the amount of TEA increasing. Si-HA particles adsorb alcohol molecules onto their surface [13–14]. These alcohol molecules are ionized into protonated alcohol and alkoxide ions are desorbed into the solution, leaving the particle positively charged in suspension which moves to Ti cathode to deposits. If there are only very few ionic charges available, they will not have sufficient force to move the particles. Therefore, the addition of TEA into suspension is in favor of EPD. The mechanism of deposition can be described as

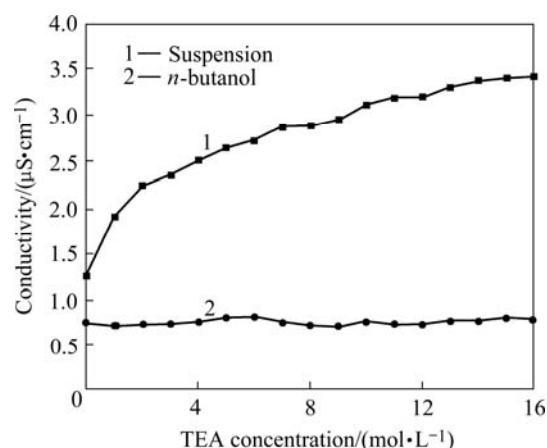
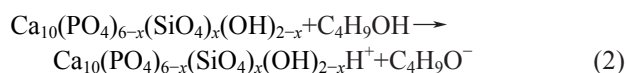
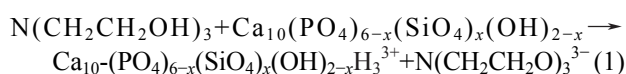


**Fig.1** Variation of electricity conductivity of suspension as function of TEA: (a) Suspension; (b) *n*-butanol

### 3.2 SEM observation

The SEM morphologies of Ti and Si-HA coatings are shown in Figs.2 and 3. Fig.2 shows the surface of titanium treated by hydrofluoric acid and nitric acid. It becomes much rougher with a lot of micro pores, which helps to increase the surface areas of substrate and form mechanical interlock between Ti and Si-HA coating. The thickness and the images of Si-HA coatings change with the variation of deposition time at a constant voltage. Fig.3 shows the morphologies of the coatings at different deposition time. It can be seen that the morphologies change from needle shape to rod-like and square shape and the rod-like fiber structures similar to bone fibers may be beneficial to the ingrowth of the coating into bone tissues. Figs.4(a) and 4(b) show the cross section morphologies of the coatings, which demonstrate that the thickness of coating changes from 8.7 μm to 24.6 μm with the variation of deposition time from 2 to 10 min.

### 3.3 Content of Si in coatings

The content of Si in the coatings was investigated by XRF and EDS and the thicknesses of coatings obtained

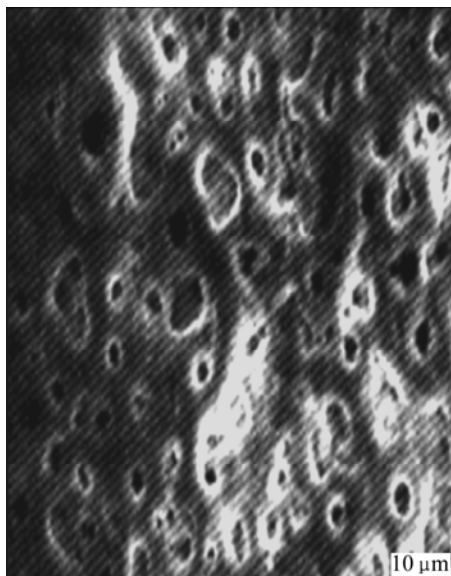


**Fig.2** SEM image of Ti surface after bioactive treatment

by SEM are listed in Table 1. The results indicate that the coatings contain elements Ca, Si, P, Ti, O and Na. The existence of Ti and Na may attribute to the  $\text{TiO}_2$  and  $\text{Na}_2\text{TiO}_3$  in the coatings. The thickness of coating changes with the deposition time as described above.

The EDS spectra of Ti/Si-HA coatings are shown in

**Table 1** Molar fraction of Si in coatings and thickness of coating

Sample	$x(\text{Si})/\%$	Deposition time/min	Thickness of coating/ $\mu\text{m}$
0.43%Ti/Si-HA	0.43	2	6.4
		4	10.8
		10	16.6
0.81%Ti/Si-HA	0.81	2	7.2
		4	13.4
		10	24.6
1.22%Ti/Si-HA	1.22	2	8.7
		4	17.8
		10	30.2

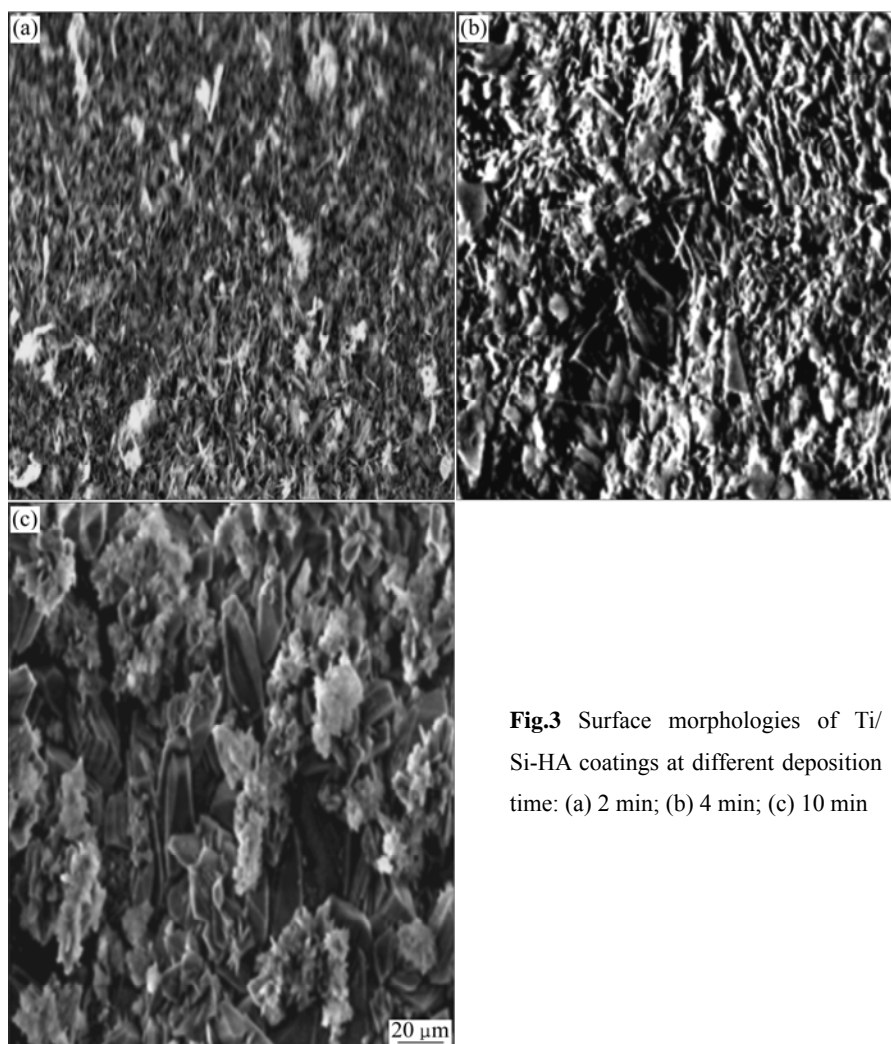


**Fig.3** Surface morphologies of Ti/Si-HA coatings at different deposition time: (a) 2 min; (b) 4 min; (c) 10 min

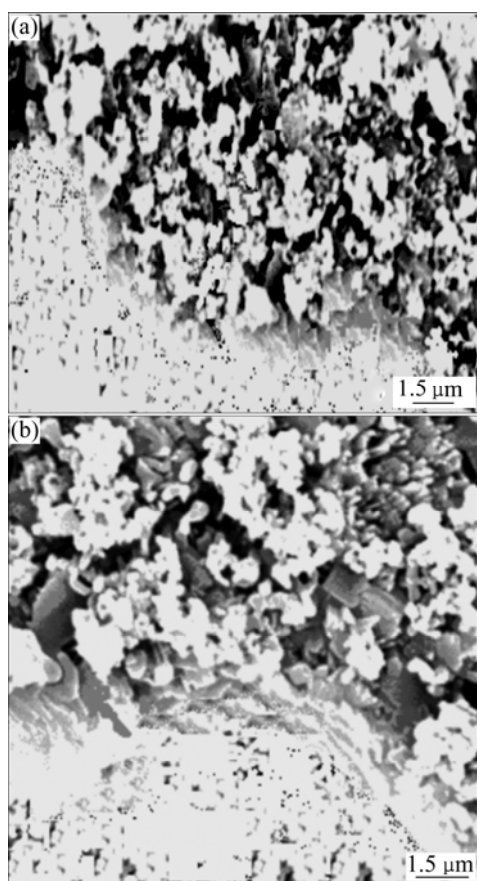


**Fig.4** Cross section morphologies of Ti/Si-HA coatings at different deposition time: (a) 2 min; (b) 10 min

Fig.5. It is indicated that silicon peaks intensify with the increase of silicon content in the suspensions. The molar fractions of Si are 0.43%, 0.81% and 1.22% for the coating prepared from suspension containing 1.9%, 3.8% and 7.2% Si, respectively. The results coupled with previous studies[8] pave the way for the fabrication of the deposits of graded composition and laminates.

### 3.4 XRD analysis

XRD patterns of Ti and Ti/HA coatings are shown

in Fig.6. After bioactive treatment, Ti substrate presents the characteristic diffraction peaks of  $\text{TiO}_2$  at  $2\theta = 25.30^\circ$ ,  $36.85^\circ$ ,  $36.85^\circ$  and  $53.90^\circ$  (JCPDS 78-2486), which suggests that  $\text{TiO}_2$  structure is formed[15]. It was reported[16] that  $\text{TiO}_2$  may enhance the bonding strength of HA coating and induce HA deposition on the substrate. XRD patterns of Ti/Si-HA coatings present the diffraction peaks of HA with no new phase being observed. A little shift toward small angle is observed with increasing the content of silicon. This indicates that the incorporation of silicon changes the lattice parameters of the crystal as reported by GIBSON et al[17]. As the radius of  $\text{P}^{5+}$  is smaller than that of  $\text{Si}^{4+}$  and the bond length of  $\text{P—O}$  (0.155 nm) is shorter than that of  $\text{Si—O}$  (0.161 nm), the radius of tetrahedrons  $\text{PO}_4^{3-}$  is smaller than that of  $\text{SiO}_4^{4-}$  and; the partial substitution of  $\text{SiO}_4^{4-}$  for  $\text{PO}_4^{3-}$  induces the shrinkage of  $a$ -axis of cell and the expansion of  $c$ -axis[18]. All of these factors result in a little change of parameter and structure of cell.

### 3.5 FTIR analysis

The FTIR spectra of HA and Si-HA coatings are presented in Fig.7. The weak hydroxyl group ( $\text{—OH}$ ) band is at  $3571\text{ cm}^{-1}$ , and  $\text{H}_2\text{O}$  band at  $3500\text{ cm}^{-1}$  and  $1648\text{ cm}^{-1}$ . The phosphate stretching vibration bands are identified by peaks at  $960$  and  $870\text{ cm}^{-1}$ , and the bending vibration band of phosphate by two peaks at  $603$  and  $567\text{ cm}^{-1}$ . Compared with the pure HA coatings, the notable effects of silicon substitution on FTIR spectra are revealed by the changes of  $\text{PO}_4^{3-}$  bands at  $960$ ,  $870$ ,  $603$  and  $567\text{ cm}^{-1}$ . The spectra show that the intensities of bands corresponding to  $\text{—OH}$  groups and  $\text{PO}_4^{3-}$  groups decrease with the silicon substitution.

### 3.6 Bond strength of coating

The bond strength of Ti/Si-HA coatings ( $x(\text{Si}) = 1.22\%$ , thickness  $30.2\text{ }\mu\text{m}$ ) with bioactively treated substrate is  $13.2\text{ MPa}$  according to the standard of GB T/

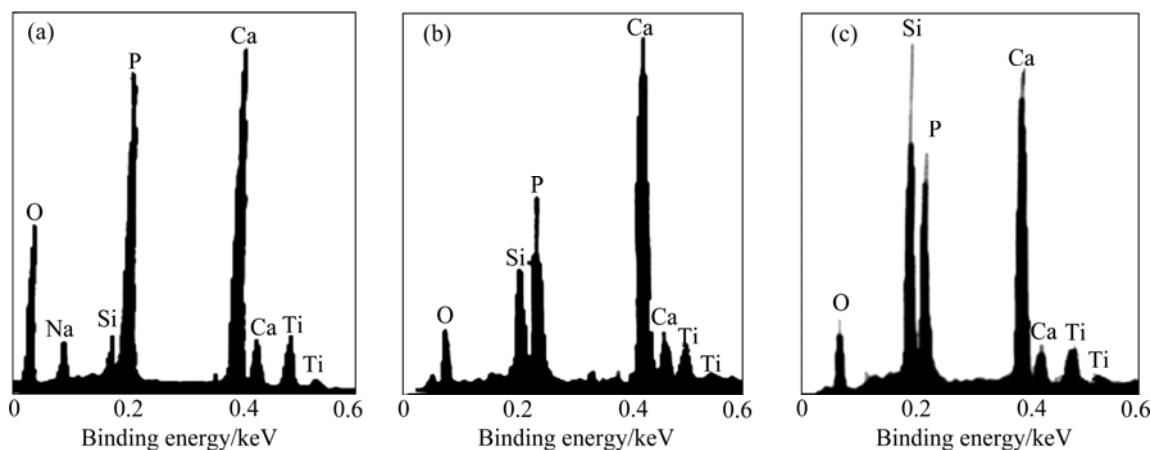


**Fig.5** EDS spectra of Ti/Si-HA coatings with different molar ratios of Si substituted in suspension: (a) 1.9%; (b) 3.8%; (c) 7.2%

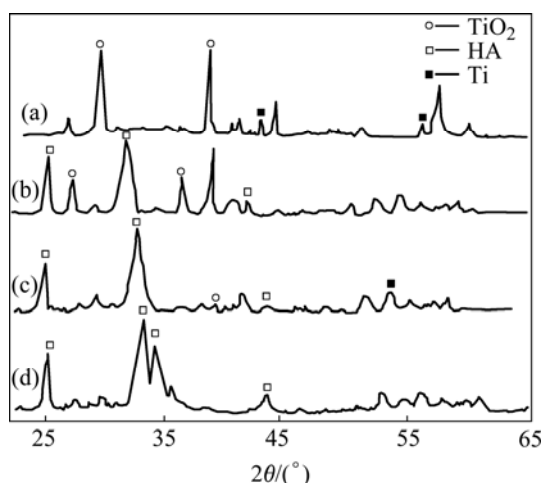


**Fig.6** XRD spectra of surface of Ti and Ti/HA coating: (a) Ti after bioactive treatment; (b) Ti/Si-HA coating (1.22% Si); (c) Ti/Si-HA coating (0.81% Si); (d) Pure Ti/HA coating

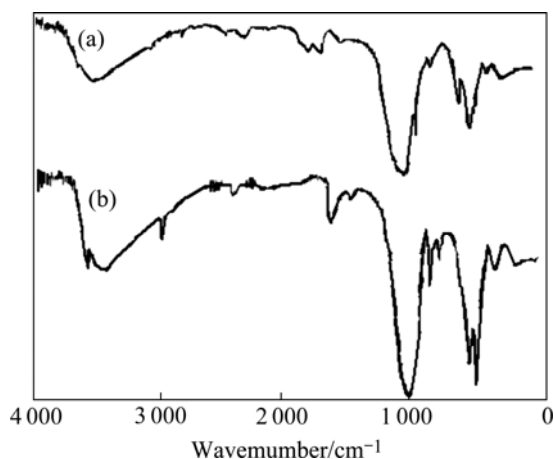


**Fig.7** FTIR patterns of Ti/Si-HA (1.22% Si) (a) and Ti/HA (b) coatings

8642—1988. By comparison, the bond strength of the coating without treatment is 6.2 MPa. Tensile strength of the coating with  $\text{TiO}_2$  as sublayer is 16.7 MPa. The formation of  $\text{TiO}_2$  and titanate layer may decrease the stress concentration and thermal expansion coefficient mismatch between coating and titanium substrate[19], which is beneficial to improving bond strength of the coatings.

### 3.7 Interaction of Ti/Si-HA coating with BSA

#### 3.7.1 SEM morphologies

The coatings appear in a different morphology (Fig.8) after interaction with BSA for 3d. The surface of the coating demonstrates hairy and wadding shape. There are many tiny needle-shape structures growing on the surface of the coating, which makes the surface arrange in order. This suggests that the protein improves the ordering of crystals in the coating, and Si-HA might dissolve in the BSA solution.  $\text{Ca}$ ,  $\text{PO}_4^{3-}$  and  $\text{SiO}_4^{4-}$  in Si-

HA coating might dissolve, adsorb and bond with BSA and reach equilibrium in certain condition[20]. As the complicated interaction between protein and HA induces the biomineralization process of Si-HA and forms the highly self-assembly structure, it will make the biomineralization samples possess the same chemical components with bone tissues.

#### 3.7.2 FTIR analysis

The FTIR spectra of scraped Ti/Si-HA powder (Fig.9) show that  $\text{PO}_4^{3-}$  band at  $962\text{ cm}^{-1}$  is noticeably

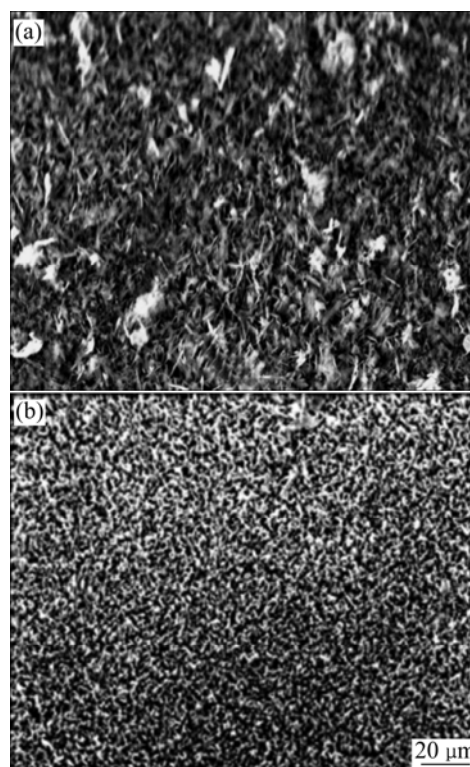


**Fig.8** SEM morphologies of Ti/Si-HA coating before (a) and after (b) reaction with BSA for 3 d

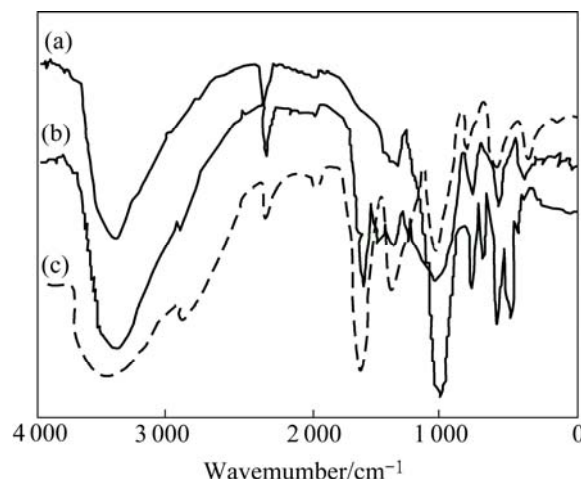


**Fig.9** FTIR patterns of Ti/Si-HA after interaction with BSA: (a) Ti/HA coating; (b) Ti/Si-HA containing 0.81% Si; (c) Ti/Si-HA containing 1.22% Si



weak, and the band of amide group ( $-\text{CONH}_2$ ) at  $1\,700\text{--}1\,600\text{ cm}^{-1}$  and the band of amide group ( $-\text{CONH}_2$ ) at  $1\,545\text{ cm}^{-1}$  in BSA[18] are observed. Compared with FTIR spectra of pure Ti/HA, the intensity of  $\text{PO}_4^{3-}$  band at  $962\text{ cm}^{-1}$  in Ti/Si-HA reduces much, and the peak of amide group ( $-\text{CONH}_2$ ) of Ti/Si-HA is more intensive. These suggest that the interaction of Ti/Si-HA coating with BSA is much greater than that of Ti/HA and the incorporation of a small amount of silicon in the HA may improve the reactive performance of Ti/HA with BSA.

## 4 Conclusions

1) The addition of TEA can increase the ionization degree of Si-HA suspension, which is in favor of the preparation of Si-HA coatings.

2) The deposit thickness and the images of Si-HA coating change with the variation of deposition time. The XRD spectra of Ti/Si-HA coating show the characteristic patterns of HA with a little shift toward small angle direction.

3) The most notable effect of silicon substitution on FTIR spectra is that the intensities of  $-\text{OH}$  and  $\text{PO}_4^{3-}$  groups decrease with the silicon substitution. Silicon dopes in the crystal lattice of HA and the content of Si in Ti/Si-HA coating rises with increasing silicon concentration in the suspensions.

4) The interaction of Ti/Si-HA coating with BSA is much greater than that of Ti/HA coating, suggesting that the incorporation of a small amount of silicon in HA is significant to improve the reactive performance of HA with protein.

## Reference

- [1] SUCHANEK W, YOSHIMURA M. Processing and properties of hydroxyapatite-based biomaterials for use as hard tissue replacement implants [J]. *J Mater Res*, 1998, 13: 94–117.
- [2] SFIDHAR T M, MUDALA U K, SUBBAIYAN M. Preparation and characterization of electrophoretically deposited hydroxyapatite coating on type 316L stainless steel [J]. *Corrosion Science*, 2003, 45: 237–252.
- [3] ZHITOM LRS K Y, GALOR L. Electrophoretic deposition of hydroxyapatite [J]. *J Mater Med*, 1997, 8: 213–219.
- [4] BALAS F, PEREZ-PARIENTE J, VALLET-REGI M. *In vitro* bioactivity of silicon-substituted hydroxyapatites [J]. *Biomaterials*, 2003, 24: 3203–3209.
- [5] TANG X L, XIAO X F, LIU R F. Structural characterization of silicon-substituted hydroxyapatite synthesized by a hydrothermal method [J]. *Materials Letters*, 2005, 59: 3841–3846.
- [6] THIAN E S, HUANG J, BEST S M, BARBER Z H. Silicon-substituted hydroxyapatite: The next generation of bioactive coatings [J]. *Materials Science and Engineering C*, 2007, 27: 251–256.
- [7] SUZUKI K, YUMURA T, MIZUGUCHI M. Apatite-silica gel composite materials prepared by a new alternate soaking process [J]. *J Sol-Gel Sci Technol*, 2001, 21: 55–63.
- [8] MONDRAGON C Z, VARGAS G G. Electrophoretic deposition of hydroxyapatite submicron particles at high voltages [J]. *Materials Letters*, 2004, 58: 1336–1339.
- [9] JUNICHI H A, YUKI A, KIYOSHI K. Fabrication of highly ordered macroporous apatite coating onto titanium by electrophoretic deposition method [J]. *Solid State Ionics*, 2004, 172: 331–334.
- [10] WEI M, RUYS A J, SWAIN M V. Interfacial bond strength of electrophoretically deposited hydroxyapatite coatings on metals [J]. *J Mater Sci: Mater Med*, 1999, 10: 401–409.
- [11] YE Qing, HU Ren, LIN Zhong-yu, LIN Chang-jian. In situ ATR-FTIR study on the interaction of HA with bovine serum albumin [J]. *Chemical Journal of Chinese Universities*, 2006, 27: 1552–1554.
- [12] DAMODARAN R, MOUDGIL B M, COLLOIDS S. Alcohols ionization function in different dispersants [J]. *Physicochem Eng Asp*, 1993, 80: 191–195.
- [13] WANG Z C, SHEMILT J, XIAO P G. Surface adsorption of alcohols on nano  $\text{Na}_2\text{TiO}_3$  [J]. *J Eur Ceram Soc*, 2002, 22: 183–188.
- [14] XIU F X, RONG F L. Effect of suspension stability on electrophoretic deposition of hydroxyapatite coatings [J]. *Materials Letters*, 2006, 60: 2627–2632.
- [15] NIWA M, WEI L, SATO I. The adsorptive property of hydroxyapatite to albumin dextrin and lipids [J]. *Biomed Mater Eng*, 1999, 9: 163–169.
- [16] TANIZAWA Y, SUZUKI T. X-ray photoelectron spectroscopy study of silicate-containing apatite [J]. *Phosphorus Res Bull*, 1994, 4: 83–88.
- [17] GIBSON I R, BEST S M, BONFIELD W. Chemical characterization of silicon-substituted hydroxyapatite [J]. *J Biomed Mater Res*, 1999, 4: 422–428.
- [18] LE VENTOURI T H, BUNACIU C E, PERDIKATIS V. Neutron powder diffraction studies of silicon-substituted hydroxyapatite [J]. *Biomaterials*, 2003, 24: 4205–4210.
- [19] TAO Wei-sun, LI Wei, JIANG Yong-Ming. The basic of protein molecules [M]. 2nd ed. Beijing: Higher Education Press, 1995. (in Chinese)
- [20] YIN Gang, ZHAN Jun, LIU Zheng. Characterization of the adsorption of bovine serum albumin on hydroxylapatite [J]. *Chemical Journal of Chinese Universities*, 2002, 22: 771–775.

(Edited by YANG Bing)